Emergent Materials
https://doi.org/10.1007/s42247-018-0009-x

ORIGINAL ARTICLE

Pollen fillers for reinforcing and strengthening of epoxy composites

Oluwatimilehin O. Fadiran[1] · Natalie Girouard[1] · J. Carson Meredith[1]

Received: 1 May 2018 / Accepted: 23 July 2018
© Springer Nature Switzerland AG 2018

Abstract

Pollen grains have the potential to be effective plant-based biorenewable fillers in polymer matrices due to their high modulus, strength, chemical stability, and unique nanoscale architectures. In this work, we present evidence for the effectiveness of pollen as a reinforcing filler in epoxy matrices, characterized as a function of pollen loading and surface treatment. Composites prepared with unmodified native defatted ragweed pollen (D) displayed decreased mechanical properties and increasing glass transition temperatures (T_g) with increasing pollen loading. A soft interphase was observed to form around native pollen that is likely due to incompletely cured epoxy, resulting in decreased mechanical properties. However, pollen treated via a common base-acid (BA) surface preparation was a load-bearing, toughening filler in epoxy composites, displaying simultaneously increased tensile strength (by 47%) and strain at break (by 70%), improving interfacial morphology (absence of soft interphase), and increasing T_g at 10 wt% pollen loading. Elastic modulus improves by 14% with 10 wt% BA pollen loading, and fitting of the modulus with the Halpin-Tsai and Counto models results in an estimated pollen exine modulus of 8 GPa, the first reported pollen modulus measurement from composite studies. Improvements in mechanical properties in BA pollen versus D pollen likely result due to crosslinks with the epoxy matrix due to the presence of protic functional groups (hydroxyls or carboxyls) on the BA surface. BA-treated ragweed pollen shows promise as a toughening filler for imparting higher strength to polymers without increasing mass.

Keywords Pollen · Polymer composite · Waterborne epoxy

1 Introduction

Polymer mechanical, thermal, and optical properties, among others, are often modified by the use of fillers [1, 2]. Filler materials for mechanical reinforcement in polymer composites range from inorganic calcium carbonate to organic carbon black and nanotubes [1–4]. It is recognized that many types of filler particulates are denser than the matrix polymer, which increases the mass of final parts. In addition, some mined inorganics and carbon-rich fillers are not produced sustainably. Due to concerns over energy efficiency deriving from mass (for example in vehicles) and increased emphasis on sustainability, there is interest in lower-density, sustainably sourced filler alternatives.

Pollen exine has the potential to be an effective biorenewable filler due to its high strength, chemical stability, low density (when hollow) and unique architecture [5–8]. Pollen is an ubiquitous natural material that is already sold as a product for medical purposes, and can be harvested in large quantities from sustainable non-food plant resources. Biologically derived particules including pollen, virus, and bacteria have attracted interest as templates for synthetic inorganic mimics that also possess properties such as magnetic forces and unique spectroscopic signatures [9–13]. Due to their complex biologically derived morphology, these mimics may provide unique function as fillers. In addition, pollen exine has been proposed as vehicles for the delivery of pharmaceuticals and vaccines [14, 15].

Pollen grains carry male gametes for plant reproduction, and they comprise an inner intine layer surrounded by a hard outer exine layer [16, 17]. The exine, composed of a substance called sporopollenin, is highly crosslinked and consists of fatty acid, phenylpropanoid, and phenolic substances. Sporopollenin is an extraordinarily stable natural organic substance [18, 19]. The monomers and macromers thought to comprise sporopollenin include aliphatic chains, aromatic cross-linkers (mainly cinnamic acids), ether cross-linkers,

Electronic supplementary material The online version of this article (https://doi.org/10.1007/s42247-018-0009-x) contains supplementary material, which is available to authorized users.

✉ J. Carson Meredith
carson.meredith@chbe.gatech.edu

[1] School of Chemical and Biomolecular Engineering, Renewable Bioproducts Institute, Georgia Institute of Technology, 311 Ferst Drive NW, Atlanta, GA 30332-0100, USA

Published online: 10 August 2018

and esters. The composition of exine should support its compatibility with relatively polar polymers. Underneath the exine, and not exposed to the outer surface, lies the cellulose-rich intine. Cellular material contained in a pollen grain can be extracted readily by using well-known preparatory methods, resulting in a strong, hollow, and clean exine shell.

Only two studies have explored pollen grains as reinforcing filler, in the thermoplastics polystyrene, polycaprolactone, and polyvinyl acetate [6, 7]. These studies showed that surface treatment and surface functionalization of pollen was critical in tuning interfacial adhesion and mechanical properties of pollen-polymer composites, in order to make pollen an effective load-bearing filler. To date, the effectiveness of pollen fillers in thermosetting polymers has remained unexplored. Epoxy resins are widely used in adhesives, coatings, composites, electric systems, and aerospace applications. Epoxy resins can be crosslinked with curing agents containing multiple amine, hydroxyl, and carboxyl groups in order to form flexible or rigid materials. Due to increased legislative restrictions on organic solvent emissions, waterborne epoxy resins are becoming increasingly important in coatings and adhesives [20]. Additionally, waterborne resins permit straightforward addition and dispersion of water-dispersible fillers.

Below, we demonstrate for the first time the successful incorporation of pollen in epoxy matrices, in particular a waterborne epoxy formulation. Short ragweed pollen (*A. artemisiifolia*) is selected as a model pollen grain because of its natural abundance, unique "spiny" echinate surface morphology, and previously published studies on composites and adhesion [21, 22]. As received, defatted pollen is compared to pollen modified by a base-acid hydrolysis. The effectiveness of pollen as a reinforcing and strengthening filler in epoxy is characterized by mechanical properties, interfacial morphology, and glass transition temperature of pollen-polymer composites as a function of pollen loading and pollen treatment.

2 Experimental section

2.1 Materials

Defatted (D) short ragweed (*A. artemisiifolia*, Greer Laboratories) pollen grains were stored at 4 °C prior to use. Potassium hydroxide (KOH, EMD Millipore) and phosphoric acid (H_3PO_4, BDH chemicals) were used for subsequent pollen cleaning and surface treatment. Epoxy resin (Air Products and Chemicals Inc., Ancarez AR555) consisted of diglycidyl ether of bisphenol-A (DGEBA) suspended at 55 wt% solids in water stabilized by a nonionic surfactant. The nominal particle size in the suspension was $D_{50} = 0.5$ μm and the epoxy has a manufacturer-reported equivalent weight (EEW) of 550. Poly(oxypropylenediamine) (Air Products and Chemicals Inc., Anquamine 401) as a 70 wt% aqueous solution, with an amine hydrogen equivalent weight (AHEW) of 200, was diluted with an equal mass of DI water to reduce the viscosity prior to use.

2.2 Pollen cellular material extraction

A base-acid treatment procedure (BA) was used to clean the exine prior to incorporation as a filler in epoxy films [5, 6, 23]. Pollen was suspended in an aqueous solution (6 *w*/*v*%) of KOH for 24 h at 25 °C under constant stirring. Following this base treatment, the pollen was washed with hot water, ethanol, and dried, and was then dispersed in 85% H_3PO_4 for 7 days at 60 °C. The pollen was washed with hot water, acetone, ethanol, and then dried. Approximately 80% of the mass of the pollen was removed during the BA treatment.

2.3 Pollen-epoxy composite film preparation

Stoichiometric amounts of epoxy and amine were mixed at room temperature with the desired amount of D or BA pollen suspended in water in order to form composites of 0–15 wt% pollen loading. The mixture was magnetically stirred for 1–5 h depending on pollen concentration, with higher concentrations mixed for longer times. The mixtures were then precured for 0.5–2 h at room temperature until the viscosity of the mixture was suitable for casting. Precuring times were determined by visual inspection and increased with pollen concentration because greater amounts of water (introduced with the pollen suspension) were present at higher pollen concentration, diluting the reactive epoxy. The mixture was cast on glass plates with a doctor blade and allowed to dry in air for a short time until the mixture is not able to flow on the substrate. Then, films were then cured for 20 min at 100 °C. Samples were peeled off the substrates using a razor. Neat epoxy was prepared using the same protocol. Both D and BA pollen were incorporated into epoxy matrices. The composite samples are labeled as follows: Epoxy with native defatted pollen (E-D) and epoxy with base-acid-treated pollen (E-BA).

2.4 Characterization

FTIR spectra were collected by using a Thermo Scientific spectrophotometer over a wavelength range of 4000 cm^{-1} to 400 cm^{-1}, for pollen grain pelletized with KBr powder. The specific surface area of D and BA pollen was determined by using adsorption of N_2 at 77 K (QuadraSorb SI, Quantachrome Inc.) and application of the BET model. Mechanical properties were measured by using a previously described high-throughput mechanical characterization

QAPCO QATAR PETROCHEMICAL COMPANY جامعة قطر QATAR UNIVERSITY

(HTMECH) instrument [24]. Polymer films were mounted between steel plates through which a steel pin contacted the film via a grid of holes 3.0 mm in diameter. The film is firmly fixed by pressure of the plates around the circumference of each hole. The pin (diameter 1.25 mm), with a hemispherical cap, deforms the film normal to the film surface at a constant strain rate (0.5 mm/s), and results in radial and tangential deflections. The resulting loading on the pin is detected by a load sensor and is quantified as an average over the results from deformations on nine holes. The loading can be used together with the pin position, hole diameter, and film thickness to determine stress-strain profiles, as described elsewhere [24]. Film thickness was determined for each sample by averaging over nine measurements with a micrometer. Uniaxial tensile testing was also performed using an Instron 5566. The samples were prepared by laser cutting films with thickness of 150 μm into 100 mm × 10 mm strips, a gage length of 80 mm was utilized, and a strain rate of 8 mm/min was used in an effort to maintain sample ratios from ASTM D882-10 to determine elastic modulus. Sample slippage was mitigated by covering the ends of samples in Kapton tape grips. A minimum of four samples were tested for each material composition where possible, and the average values were reported. Mechanical measurements were performed at ambient condition. Scanning electron microscopy (SEM) was performed (Zeiss Ultra-60 FE-SEM) to determine the interfacial morphology of freeze-fractured and HTMECH fracture surfaces of the composites. AFM contact mode and force modulation scans of composite cross sections were made with a Veeco AFM Dimension 3100. Differential scanning calorimetry (DSC) measurements were performed with a TA Instruments DSC Q200 in a nitrogen atmosphere, using specimens of 8–9 mg cut from films and sealed in aluminum pans with lids. Samples were heated from 10 to 150 °C, above T_g of the neat epoxy, at 20 °C/min, kept isothermal for 1 min, cooled down to 10 °C at 20 °C/min, and held isothermal for 1 min again. This cycle was repeated twice. T_g values were taken from the second cycle from the onset value of the tangents on the heat flow curves. The density of materials was assessed by pycnometry in a 25-ml specific gravity bottle. Ethanol was used to determine the density of D pollen, BA pollen, neat epoxy, and composites. A known mass of material, m_s, was added to the volumetric flask of known mass (m_0). The liquid of known density was then added to the flask up to the graduation marking and the total mass, m_T, is measured. The density of the solid is given by:

$$\rho_s = m_s / \left(V - \frac{m_T - m_0 - m_s}{\rho_{H2O}} \right) \quad (1)$$

where V is the volume of the flask.

3 Results and discussion

3.1 FTIR analysis

Figure 1 shows the FTIR spectra of D pollen, D pollen recovered from the epoxy suspension (with no added amine) (D-Epoxy), BA pollen, and BA pollen recovered from the epoxy suspension (BA-Epoxy). Exposure to the epoxy suspension without amine was performed to explore interactions between the epoxide and the pollen. The pollen intine in D pollen contributes a cellulose fingerprint spectrum in the 1100 to 900 cm^{-1} region of the pollen intine [19, 25]. The spectrum for BA pollen lacks peaks associated with polysaccharides in this range, indicating the removal of the intine, in agreement with prior work [5, 6, 26]. D pollen also exhibits a broad band at 3393 cm^{-1} due to O-H stretching that shows a stronger intensity than the –CH stretches of $–CH_2$ groups at 2930 and 2855 cm^{-1}. In contrast, BA pollen displays a more narrow –OH band with a smaller intensity than the $–CH_2$ peaks. BA pollen's OH band is also shifted to higher wavenumbers around 3433 cm^{-1}, indicating increased fractions of free hydroxyls. The C=O stretch of carboxyl groups also shifts from 1674 to 1706 cm^{-1} in D and BA pollen, respectively. Therefore, the BA treatment results in a decreased ratio of

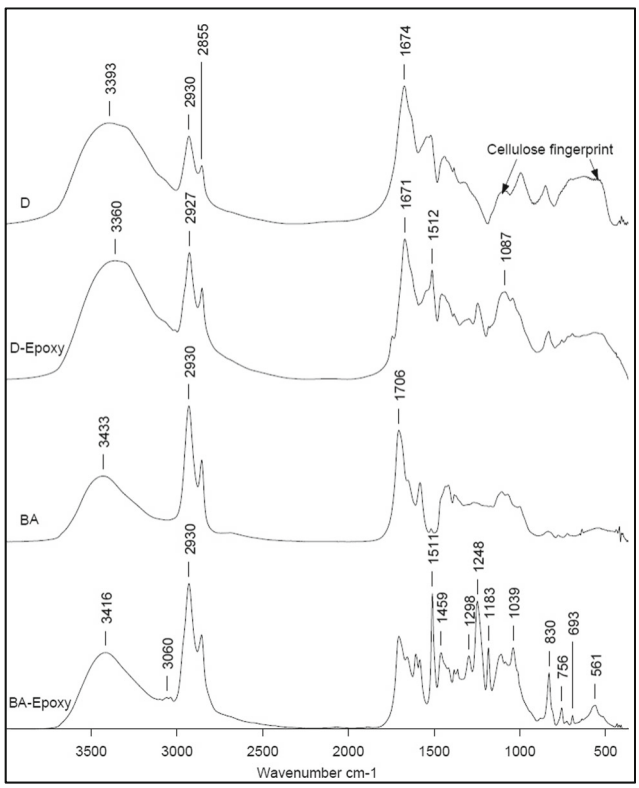

Fig. 1 FTIR spectra of D and BA pollen before and after recovery from epoxy suspension (D-Epoxy, BA-Epoxy)

hydroxyl to methylene moieties, likely due to hydrolysis of the cellulosic intine, and results in increased fractions of free hydroxyl and carboxyl groups in or on the sporopollenin exine. Additionally, additional hydroxyl groups may be generated on the pollen surface due to phosphorylation of hydroxyls and/or carboxyls [5]. These results are consistent with previously reported measurements from our group as well, including zeta potentials of BA-treated pollen that indicate negative and pH-sensitive acidic groups on the surface [6].

BA-Epoxy displays several additional peaks versus BA pollen, indicating the strong interactions between BA pollen and epoxy. Peaks associated with the epoxide group appear at 3060 cm^{-1} due to C-H stretching and at 830 cm^{-1} due to C-O-C stretching [27]. C-H stretches of aromatic groups in the epoxy molecules appear as a shoulder peak at 2925 cm^{-1} [27–29]. The C-C stretching of aromatics also appears at 1511 cm^{-1} and the C=C stretching of aromatic groups appears at 1459 cm^{-1} [27, 28, 30]. C-O-C stretching of epoxy ether groups appears at 1248 cm^{-1} and 1039 cm^{-1} [27–29]. Many of these peaks are lacking in D-Epoxy, and where new peaks are visible (1511 cm^{-1} and 1246 cm^{-1}), they are relatively weak signals. The higher intensity of peaks and presence of numerous new peaks on BA-Epoxy versus D-Epoxy may be due to higher fractions of free hydroxyl and carboxyl groups more accessible for surface interactions on BA pollen versus D pollen. It is possible that the epoxide reacted with pollen surface hydroxyls or carboxyls, forming covalent linkages between the pollen and the epoxy matrix Fig. 1, shows that between BA and BA-Epoxy, the ratio of –OH (~ 3400 cm^{-1}) groups to $–CH_2$ (2930 cm^{-1}) is unchanged, while the ratio of –COOH (1706 cm^{-1}) to both –OH and $–CH_2$ decreases. This may indicate the preferential participation of carboxyl groups in reaction with epoxide.

3.2 Interfacial morphology

Figure 2 presents the SEM images of freeze-fractured and HTMECH fracture surfaces of E-D films. Both freeze fracture (Fig. 2a–d) and HTMECH fracture surfaces (Fig. 2e, f) show intimate contact between the pollen and the epoxy matrix in

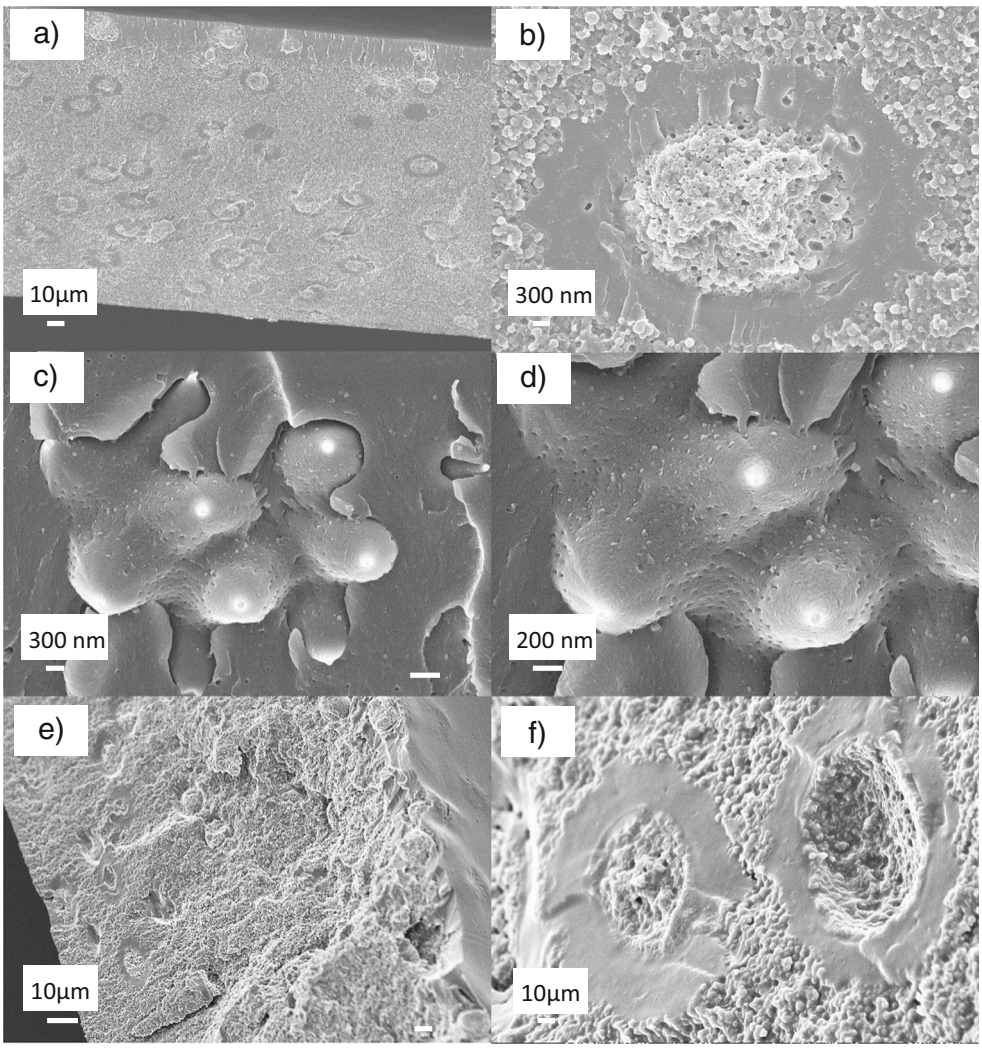

Fig. 2 E-D fracture surfaces. Freeze-fractured cross sections (**a**–**d**) and HTMECH fracture surfaces (**e**, **f**) at 10 wt% pollen loading

general. However, a visible interphase of ~ 1 μm in thickness can be seen surrounding the D pollen. Where intact D pollen grains can be found (Fig. 2c, d), interfacial voids are present. It can also be observed that only small amounts of epoxy attach to the surface and pores of D pollen, indicated by the visibility of pollen pores. With both fracture surfaces, the majority of D pollen grains are broken within the exine shell structure, indicating some degree of adhesion between the two phases.

Figure 3 presents the SEM images of freeze-fractured and HTMECH fracture surfaces of E-BA films. Both freeze fracture (Fig. 3a–d) and HTMECH fracture surfaces (Fig. 3e, f) reveal intimate contact between pollen grains and the epoxy matrix. Additionally, E-BA films lack the visible interphases that were present with E-D films. Also, in contrast to D pollen, where intact BA pollen can be found (Fig. 3b, c), its surface is clearly coated with layers of epoxy. The interface between the pollen outer surface and the epoxy matrix is virtually indistinguishable. Again, the pollen grains that are visible are almost always broken cross sections of BA pollen due to some degree of adhesion between the epoxy matrix and BA pollen outer surface. The surface area of the BA pollen is about 3× that of D pollen, 5.8 m^2/g versus 2.0 m^2/g, respectively, largely reflecting the cleaning of pore spaces in the sporopollenin shell. The epoxy apparently is able to enter the hollow shells (arrows in Fig. 3e, f) through these pores, which may have two interesting outcomes. First, this epoxy may be shielded from stresses experienced outside the grain during deformation. This is referred to as "occluded polymer". Second, it is evident that the epoxy within the shells displays more air gaps than that of the matrix (arrows in Fig. 3e, f). Thus, BA pollen introduces a greater amount of air into the final material than D pollen or the unfilled epoxy. This is consistent with the BA pollen being essentially hollow. D and BA pollens recovered from epoxy suspension without amine added are shown in Fig. S2 and Fig. S3 (supporting information). D-Epoxy is covered with a thick coating of uncrosslinked epoxy which is smooth in appearance, similar to the thick interphases in Fig. 2 and the fracture surface of a purely epoxy film (Fig. S4, supporting information). BA-Epoxy had a thinner, rougher coating with more epoxy spheres intact. The coatings on

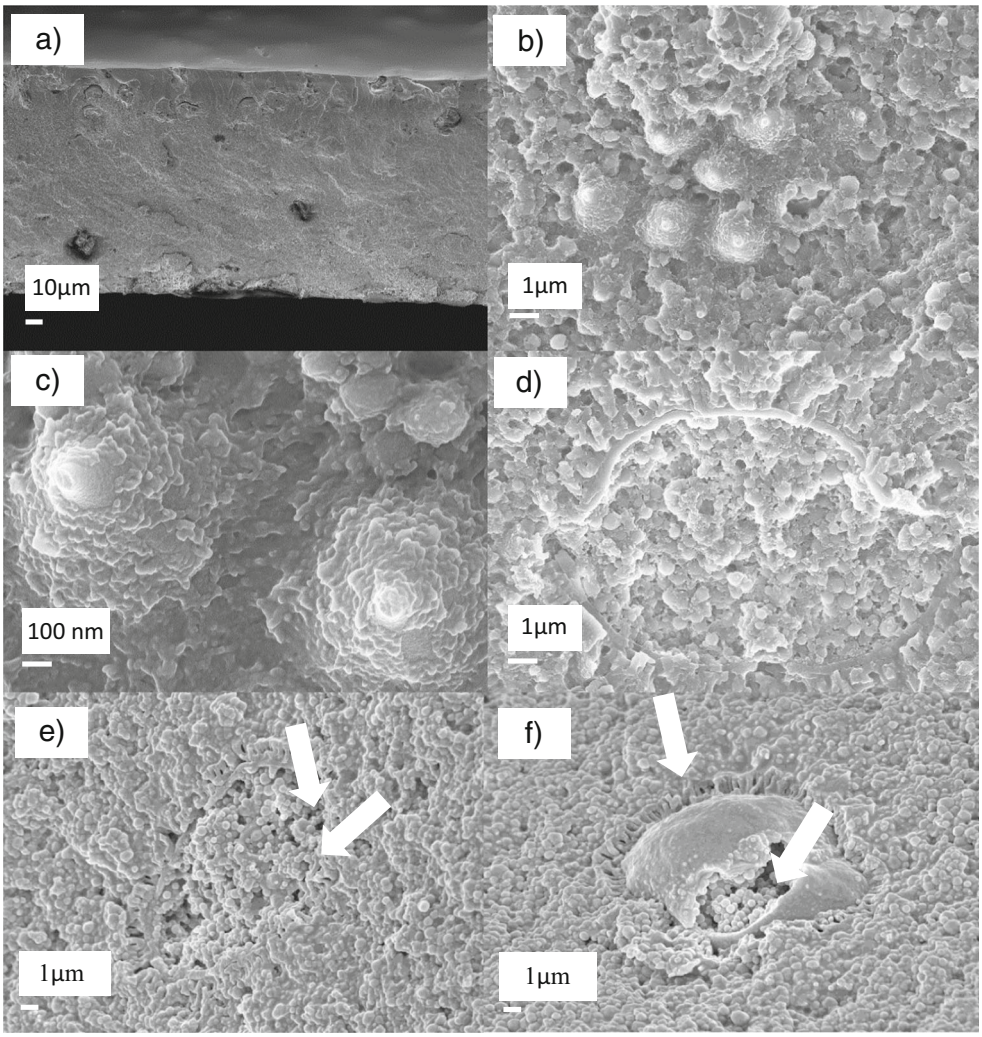

Fig. 3 E-BA fracture surfaces. Freeze-fractured cross sections (**a**–**d**) and HTMECH fracture surfaces (**e**, **f**) at 10 wt% pollen loading. Arrows indicate epoxy within pollen grains and additional air gaps

BA-Epoxy surfaces (especially the inner surface, Fig. S3d) more clearly mirror the morphology of the crosslinked bulk epoxy matrix seen in Figs. 2 and 3. The non-coalesced epoxy spheres may occur due to crosslinking reaction kinetics of the waterborne epoxy, where the epoxy particle morphology is maintained because the crosslinking reaction is faster than the coalescence of the epoxy particles. Therefore, the intact epoxy particle morphology indicates successful crosslinking. This means that BA pollen, which displays the intact particle morphology especially on its inner surface, has the ability to crosslink with epoxy (without amine) due to its polar functionalities. Conversely, D pollen may be unable to crosslink with epoxy due to its relatively lower amount as –OH, indicated in the FTIR in Fig. 1.

D pollen may also affect the crosslinking ability of the amine. The supernatant of amine solutions mixed with D pollen displays a strong color shift, from yellow to dark brown (Fig. S5, supporting information). In the BA pollen mixtures, where intracellular material is absent, no color shift occurs. D pollen mixed with only water extracted some intracellular material, but still remained essentially clear, so extracted intracellular material alone does not account for the strong color shift. Films cured with unaltered amine and the altered D-amine immediately after mixture were transparent. However, films cured with D-amine after 3 days became opaque (Fig. S6). It is well known that amines can strongly bind to lipid structures, such as phospholipids and cellulose, which are present in D pollen intracellular material within the D pollen [31–33]. One potential explanation is that the intracellular material is released from within the pollen grain and strongly binds with the amine crosslinker overtime, a possibility to be explored below.

3.4 Mechanical properties

Figure 4 shows mechanical properties for both E-D and E-BA films with HTMECH. The error bars are 95% confidence intervals. Elastic modulus, tensile strength, and strain at break all decreased continuously with the increased loading of D pollen. Considering the interfacial morphology of E-D films, this may be due to the visible uncrosslinked interphase present in these films. An uncrosslinked interphase would be softer than the bulk matrix. Thus, with increasing pollen loading, the material is increasingly softened and efficient stress transfer between the phases is impaired, effectively decreasing material stiffness and strength with increased pollen loading. In contrast, elastic modulus, tensile strength, and strain at break all simultaneously increase with the increased loading of BA pollen. Versus neat epoxy, composites containing BA pollen showed increased modulus (~ 17% increase), tensile strength (86% increase), and strain at break (73% increase). As discussed above, E-BA films did not display a visible interphase, attributed to uncrosslinked epoxy in D pollen. Thus,

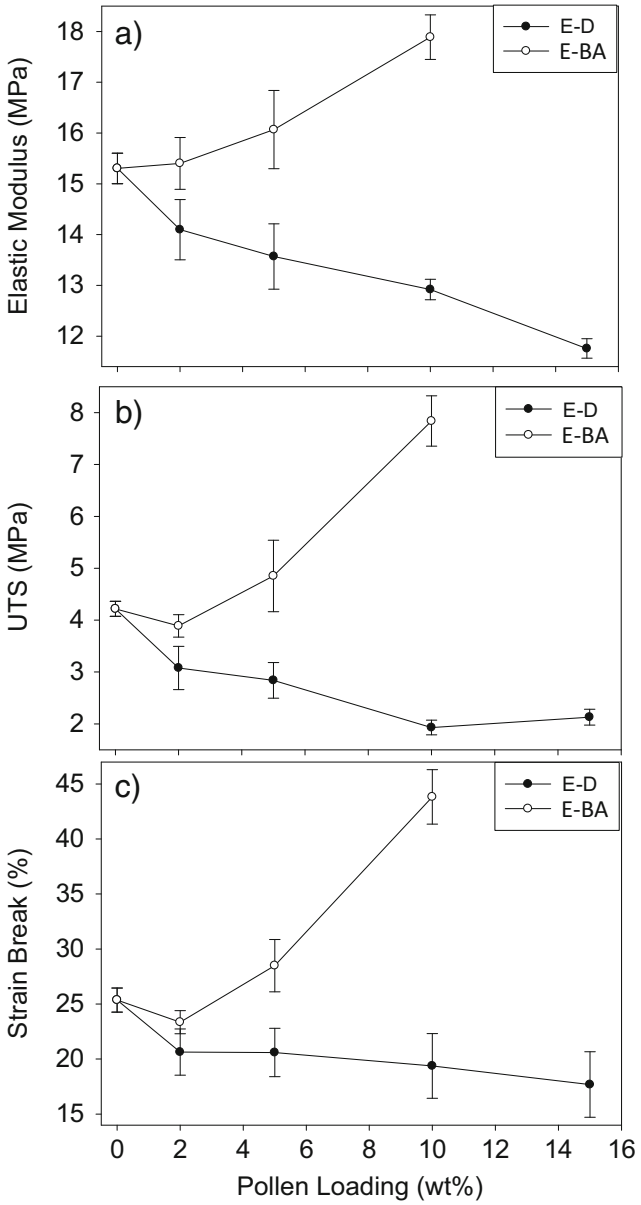

Fig. 4 Elastic modulus (**a**), UTS (**b**), and strain at break (**c**) of both E-D and E-BA composites measured with HTMECH under biaxial tension. The error bars are 95% confidence intervals

BA pollen likely forms a stronger more interconnected interphase with epoxy than D pollen, because it is able to crosslink with epoxy molecules. The mechanical results suggest that there is a high degree of adhesion between the BA pollen and the epoxy matrix, resulting in efficient stress transfer between the phases, further supporting the presence of crosslinking between BA pollen and epoxy. These mechanical observations and the proposed crosslinking driving adhesion are also consistent with the SEM evidence of strongly attached epoxy to the BA pollen surface (Fig. 3b–e) and BA pollen recovered from epoxy solutions (Fig. S3, supporting information). In a previous study with polyvinyl acetate [6], a surface functionalization with an organosilane coupling agent

was required to optimize interfacial adhesion and achieve simultaneous increases in all mechanical properties. Crosslinking between surface –OH groups, the epoxide, and the epoxy matrix eliminates the need for an additional functionalization step. These results indicate that pollen is more compatible with epoxy than with previous thermoplastics that were studied [6, 7].

The stiffening effects observed in E-BA films (Fig. 4) indicate that the pollen exine shell has a higher inherent modulus than the epoxy matrix, although independent measurements of exine modulus are not available. Only one study reported the modulus of pollen, measured by compressing single dessicated ragweed grains [8]. The result, given as E_h, a product of exine thickness and compressive modulus, was 1653 N/m [8]. This value can be converted into a compressive modulus by dividing by wall thickness. For a nominal 1-μm-thick exine wall, the modulus would be 1650 MPa. Modulus measurements from the composites can be used to extract modulus estimates for the pollen filler through the fitting of composite models to the experimental data. Because the HTMECH modulus values are derived as a simple slope from the complex loading of a thin film normal to its surface, the moduli in Fig. 4a are not suitable for determination of a modulus that can be compared in magnitude to the uniaxial tensile tests usually used. Thus, we measured elastic moduli for composites by using a conventional uniaxial geometry on an Instron 5566. The results are shown in Fig. 5a, indicating the same trends as the HTMECH moduli in Fig. 4a, but at a magnitude usually associated with epoxy materials. In particular, these measurements confirm independently from Fig. 4a that the modulus increases when E-BA is added and decreases when E-D is added, indicating the important effect of surface treatment.

We used two models of two-phase composites to estimate the pollen modulus from the data for the well-adhered BA pollen composites in Fig. 5a. The Halpin-Tsai [34] semi-empirical model is shown in Eqs. 3–5.

$$E_c = E_m\left(\frac{1+\eta\zeta V_f}{1-\eta V_f}\right) \tag{2}$$

ζ and η are expressed as:

$$\zeta = 2 + 40{V_f}^{10} \tag{3}$$

$$\eta = \frac{\frac{E_f}{E_m}-1}{\frac{E_f}{E_m}+\zeta} \tag{4}$$

Here, E_c is the composite modulus, E_m is the epoxy matrix modulus (at 0% pollen), and E_f is the filler (pollen) modulus that is determined by least-squares regression of Eq. 2 to the data. V_f is the filler (pollen) volume fraction. In addition to the Halpin-Tsai model, the Counto model was used to fit the

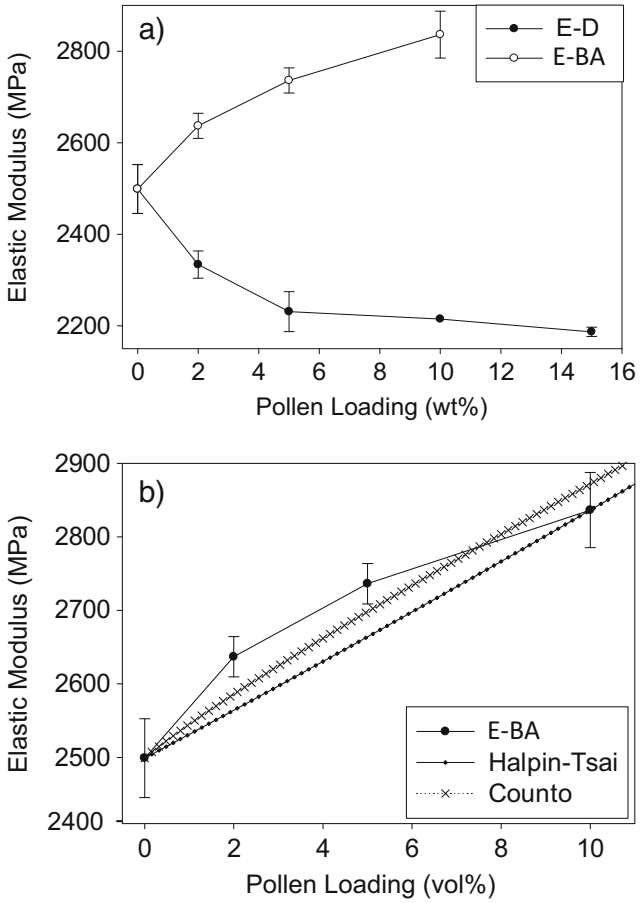

Fig. 5 **a** Elastic modulus for E-BA and E-D pollen composites with epoxy measured from uniaxial tension experiments. The error bars are 95% confidence intervals. **b** Fitting of elastic modulus of E-BA from (**a**) with two models for filled polymers

Instron experimental data. The Counto model [35, 36], shown in Eq. 5, considers a two-phase composite and assumes perfect adhesion between matrix and filler.

$$E_c = E_m\left[1 + V_f/\left(\sqrt{V_f}-V_f+\frac{E_m}{E_f-E_m}\right)\right] \tag{5}$$

As shown in Fig. 5b, a better fit is provided by the Counto model. The largest percent errors were 2.7% and 1.8% for the Halpin-Tsai and the Counto model respectively. The Halpin-Tsai model resulted in a fitted modulus of 8170 MPa and the Counto model returned a fitted modulus of 8005 MPa for BA pollen versus the measured 2499 MPa of the neat epoxy polymer. Thus, modeling indicates that ragweed pollen has a high modulus value, exceeding the neat epoxy by a factor of 3.2, supporting its utility as a reinforcing filler.

3.5 Thermal properties

The glass transition temperature was determined for the E-D and E-BA films, and is reported in Fig. 6. It is clear that in both E-D and E-BA films, the T_g increases with increased pollen loading,

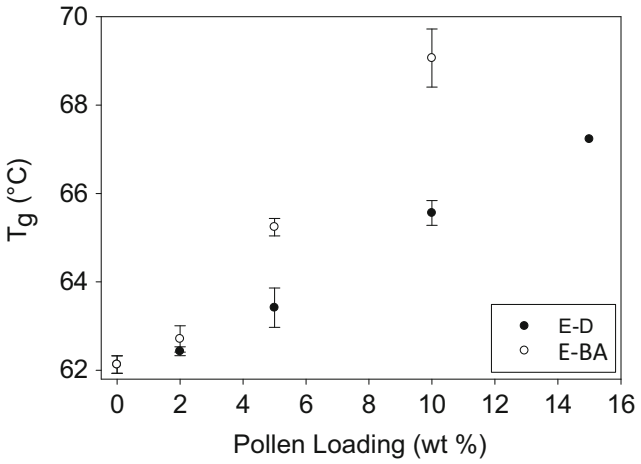

Fig. 6 Glass transition (T_g) of pollen-epoxy composites as a function of pollen loading

suggesting restriction of epoxy chains surrounding pollen surfaces [37, 38]. This correlates with the observed interfacial and mechanical properties observed in the films. Comparing E-D and E-BA films, it is observed that T_g values in E-BA films are higher than T_g values in E-D films at similar pollen loadings. For example, at 10 wt% pollen loading, E-D film displays a T_g of 65.4 °C and E-BA displays a T_g of 69.1 °C. This suggests a higher restriction of epoxy chains in E-BA films. The soft uncrosslinked interphase likely causes the less enhanced T_g value. Due to lack of a soft interphase in D pollen composites and crosslinking with epoxy, BA pollen is able to elevate the T_g more significantly. These results correspond well with FTIR peaks of higher intensity on BA pollen recovered from epoxy solution than D pollen and improved mechanical properties of E-BA films. Again, these results indicate that pollen-filled epoxies show improved compatibility versus previous thermoplastics [6, 7]. Previously, T_g of polyvinyl acetate was not altered significantly with increased pollen loading, even after surface treatment and functionalization. However, with epoxy, even prior to any surface treatments, D pollen is able to elevate T_g, indicating improved matrix compatibility.

3.6 Density of materials

The density of D pollen was measured with pycnometry to be 1.305 g/cm^3, and the BA pollen density was found to be 1.165 g/cm^3. Intracellular material in D pollen likely makes it denser than hollow BA-treated pollen. However, native D pollen was considerably less dense than some widely used mineral-based fillers, such as talc ($\rho = 2.75$ g/cm^3) and calcium carbonate ($\rho = 2.71$ g/cm^3), and the density of D pollen is closer to those of carbon nanotubes ($\rho = 1.3$–1.4 g/cm^3), cellulose ($\rho = 1.5$ g/cm^3), and starch ($\rho = 1.5$ g/cm^3). The shells of BA-treated pollen have a lower density than all of these fillers. The pycnometry method was also used to determine the neat epoxy and pollen-epoxy composite densities. Neat epoxy's density was measured as 1.214 g/cm^3, comparable to previously measured densities of epoxy [39].

E-D and E-BA film densities were determined to be 1.208 g/cm^3 and 1.221 g/cm^3, respectively. Thus, unlike many inorganic fillers, pollen does not significantly increase the density of the epoxy matrix. BA pollen decreased the material density by ~0.5% at a 10 wt% loading versus neat epoxy. However, E-BA mechanical properties appear to still be increasing at 10 wt% pollen loading. Thus, it is likely that further decreases in density are possible while still enhancing the mechanical properties of the cured epoxy. Also, interesting future work may involve sealing BA pollen and trapping air within the shells, which would allow for larger density reductions.

4 Conclusion

The efficacy of ragweed pollen as a filler on the thermal, interfacial, and mechanical properties of epoxy-pollen composites was investigated. Composites prepared with as received ragweed pollen (D) displayed decreased mechanical properties with increasing pollen loading due to the presence of a soft interphase. D pollen is unable to crosslink with epoxy, likely due to a lower amount of protic functional groups on the exine surface. However, D pollen composites still showed increased glass transition temperatures (T_g) with increasing pollen loading. Pollen treated via a base-acid (BA) surface preparation becomes a load-bearing filler in epoxy, displaying simultaneous stiffening and strengthening coupled with an improved interfacial morphology and increased T_g with increasing pollen loading. Modeling the elastic modulus gains with both the Halpin-Tsai and Counto models resulted in an estimated pollen exine modulus of 8 GPa, the first reported pollen modulus measurement from composite studies. Improvements in mechanical properties in BA pollen versus D pollen likely result due to crosslinks with the epoxy matrix due to the presence of protic functional groups (hydroxyls or carboxyls) on the BA surface. BA pollen displayed higher compatibility with epoxy than with the thermoplastics previously studied (polystyrene, polycaprolactone, and polyvinyl acetate) [6, 7], and with no additional surface functionalization step. Finally, BA pollen was found to lower slightly the composite density relative to neat epoxy. These results indicate that pollen is a promising filler for creating high strength, light-weight polymer composites and merits further study, for example, investigating additional matrices with potential compatibility with pollen or incorporating pollen of different species in polymers in order to elucidate the effect of filler microstructure on the wetting and adhesion of fillers.

QAPCO QATAR PETROCHEMICAL COMPANY
جامعة قطر QATAR UNIVERSITY

Funding information We would like to thank the Renewable Bioproducts Institute (Georgia Institute of Technology) and the Air Force Office of Scientific Research (Grant # FA9550-10-1-0555) for financial support of this research.

References

1. S.-Y. Fu, X.-Q. Feng, B. Lauke, Y.-W. Mai, Effects of particle size, particle/matrix interface adhesion and particle loading on mechanical properties of particulate–polymer composites. Compos. Part B **39**, 933–961 (2008)
2. G. Wypych, *Handbook of fillers, 3 edn* (ChemTec, 2010)
3. B.J. Ash, D.F. Rogers, C.J. Wiegand, L.S. Schadler, R.W. Siegel, B.C. Benicewicz, T. Apple, Mechanical properties of Al2O3/polymethylmethacrylate nanocomposites. Polym. Compos. **23**, 1014–1025 (2002)
4. Z. Spitalsky, D. Tasis, K. Papagelis, C. Galiotis, Carbon nanotube–polymer composites: chemistry, processing, mechanical and electrical properties. Prog. Polym. Sci. **35**, 357–401 (2010)
5. S. Barrier, Physical and chemical properties of sporopollenin exine particles, Ph.D. Thesis, University of Hull, (2008)
6. O.O. Fadiran, J.C. Meredith, Surface treated pollen performance as a renewable reinforcing filler for poly(vinyl acetate). J. Mater. Chem. A **2**, 17031–17040 (2014)
7. J.H. Lee, B.M. Suttle, H.J. Kim, J.C. Meredith, Pollen: a novel, biorenewable filler for polymer composites. Macromol. Mater. Eng. **296**, 1055–1062 (2011)
8. T. Liu, Z. Zhang, Mechanical properties of desiccated ragweed pollen grains determined by micromanipulation and theoretical modelling. Biotechnol. Bioeng. **85**, 770–775 (2004)
9. B. Goodwin, I. Gomez, Y. Fang, J.C. Meredith, K.J. Sandhage, Conversion of pollen particles into three-dimensional ceramic replicas tailored for multimodal adhesion. Chem. Mater. **25**, 4529–4536 (2013)
10. W.B. Goodwin, D. Shin, D. Sabo, S. Hwang, Z.J. Zhang, J.C. Meredith, K.H. Sandhage, Bioinspiration & Biomimetics **12**, 066009 (2017)
11. Y. Wang, Z.M. Liu, B.X. Han, Y. Huang, G.Y. Yang, Carbon microspheres with supported silver nanoparticles prepared from pollen grains. Langmuir **21**, 10846–10849 (2005)
12. Y. Wang, Z.M. Liu, B.X. Han, Z.Y. Sun, J.M. Du, J.L. Zhang, T. Jiang, W.Z. Wu, Z.J. Miao, Chemical communications, 2948–2950 (2005)
13. H.S. Lin, M.C. Allen, J. Wu, B.M. DeGlee, D. Shin, Y. Cai, K.H. Sandhage, D.D. Deheyn, J.C. Meredith, Chem Mater **27**, 7321–7330 (2015)
14. S.U. Atwe, Y.Z. Ma, H.S. Gill, Pollen grains for oral vaccination. J. Control. Release **194**, 45–52 (2014)
15. I. Sargin, L. Akyuz, M. Kaya, G. Tan, T. Ceter, K. Yildirim, S. Ertosun, G.H. Aydin, M. Topal, Controlled release and antiproliferative effect of imatinib mesylate loaded sporopollenin microcapsules extracted from pollens of Betula pendula. Int. J. Biol. Macromol. **105**, 749–756 (2017)
16. P. Piffanelli, J.H.E. Ross, D.J. Murphy, Biogenesis and function of the lipidic structures of pollen grains. Sex. Plant Reprod. **11**, 65–80 (1998)
17. R. Wiermann, S. Gubatz, Pollen wall and sporopollenin. Int. Rev. Cytol. **140**, 35–72 (1992)
18. S. Blackmore, A.H. Wortley, J.J. Skvarla, J.R. Rowley, Pollen wall development in flowering plants. New Phytol. **174**, 483–498 (2007)
19. E. Dominguez, J.A. Mercado, M.A. Quesada, A. Heredia, Sex. Plant Reprod. **12**, 171–178 (1999)
20. E.M. Petrie, *Epoxy adhesive formulations* (McGraw-Hill, 2006)
21. H. Lin, I. Gomez, J.C. Meredith, Pollenkitt wetting mechanism enables species-specific tunable pollen adhesion. Langmuir **29**, 3012–3023 (2013)
22. B.J.R. Thio, J.H. Lee, J.C. Meredith, Characterization of ragweed pollen adhesion to polyamides and polystyrene using atomic force microscopy. Environ. Sci Technol. **43**, 4308–4313 (2009)
23. F. Zetzsche, H. Vicari, Untersuchungen über die Membran der Sporen und Pollen II. Lycopodium clavatum L. 2. Helv Chim Acta **14**, 58–78 (1931)
24. J.L. Sormana, S. Chattopadhyay, J.C. Meredith, Rev. Sci. Instrum. **76** (2005)
25. E. Dominguez, J.A. Mercado, M.A. Quesada, A. Heredia, Isolation of intact pollen exine using anhydrous hydrogen fluoride. Grana **37**, 93–96 (1998)
26. G. Shaw, D.C. Apperley, 13C-NMR spectra ofLycopodium clavatumsporopollenin and oxidatively polymerised β-carotene. Grana **35**, 125–127 (1996)
27. J.C.C. Maria González González, J.C. Cabanelas, J. Baselga, in *Infrared spectroscopy - materials science, engineering and technology*, ed. by T. Theophile. (InTech, 2012), pp. 261–284
28. V. Cecen, Y. Seki, M. Sarikanat, I.H. Tavman, FTIR and SEM analysis of polyester- and epoxy-based composites manufactured by VARTM process. J. Appl. Polym. Sci. **108**, 2163–2170 (2008)
29. S.H. Xu, N. Girouard, G. Schueneman, M.L. Shofner, J.C. Meredith, Mechanical and thermal properties of waterborne epoxy composites containing cellulose nanocrystals. Polymer **54**, 6589–6598 (2013)
30. J.I. Yang, Part I: synthesis of aromatic polyketones via soluble precursors derived from bis(A-amininitrile)s Part II: modifications of epoxy resins with functional hyperbranched poly(areylene ester)s, Ph.D. Thesis, Virginia Tech, (1998)
31. M. Amato, F. Barbato, P. Morrica, F. Quaglia, M.I. La Rotonda, Helv Chim Acta **83**, 2836–2847 (2000)
32. J.Y.C. Ma, J.K.H. Ma, K.C. Weber, Fluorescence studies of the binding of amphiphilic amines with phospholipids. J. Lipid Res. **26**, 735–744 (1985)
33. B. Tadolini, G. Hakim, Ital. J. Biochem. **37**, A184–A185 (1988)
34. J.C. Halpin, J.L. Kardos, Polym. Eng. Sci. **16**, 344–352 (1976)
35. S. Ahmed, F.R. Jones, A review of particulate reinforcement theories for polymer composites. J. Mater. Sci. **25**, 4933–4942 (1990)
36. U.J. Counto, The effect of the elastic modulus of the aggregate on the elastic modulus, creep and creep recovery of concrete. Mag. Concr. Res. **16**, 129–138 (1964)
37. H.B. Lu, S. Nutt, Restricted relaxation in polymer nanocomposites near the glass transition. Macromolecules **36**, 4010–4016 (2003)
38. A. Yim, R.S. Chahal, L.E. Stpierre, The effect of polymer—filler interaction energy on the T′g of filled polymers. J. Colloid Interface Sci. **43**, 583–590 (1973)
39. A. Yasmin, J.L. Abot, I.M. Daniel, Processing of clay/epoxy nanocomposites by shear mixing. Scr. Mater. **49**, 81–86 (2003)